RNA-Seq Analysis Illuminates the Early Stages of *Plasmodium* Liver Infection

Maria Toro-Moreno[a,*], Kayla Sylvester[b,*], Tamanna Srivastava[a], Dora Posfai[b], and Emily R. Derbyshire[a,b,#]

[a] Department of Chemistry, Duke University, Durham, NC, USA

[b] Department of Molecular Genetics and Microbiology, Duke University, Durham, NC, USA

Running Head: *Plasmodium* liver stage transcriptome

#Address correspondence to Emily R. Derbyshire, emily.derbyshire@duke.edu.

*Authors contributed equally.

ABSTRACT

The apicomplexan parasites *Plasmodium* spp. are the causative agents of malaria, a disease that poses a significant global health burden. *Plasmodium* spp. initiate infection of the human host by transforming and replicating within hepatocytes. This liver stage (LS) is poorly understood when compared to other *Plasmodium* life stages, which has hindered our ability to target these parasites for disease prevention. We conducted an extensive RNA-seq analysis throughout the *Plasmodium berghei* LS, covering as early as 2 hours post infection (hpi) and extending to 48 hpi. Our data revealed that hundreds of genes are differentially expressed at 2 hpi, and that multiple genes shown to be important for later infection are upregulated as early as 12 hpi. Using hierarchical clustering along with co-expression analysis, we identified clusters functionally enriched for important liver-stage processes such as interactions with the host cell and redox homeostasis. Furthermore, some of these clusters were highly correlated to the expression of ApiAP2 transcription factors, while showing enrichment of mostly uncharacterized DNA binding motifs. This finding presents potential LS targets for these transcription factors, while also hinting at alternative uncharacterized DNA binding motifs and transcription factors during this stage. Our work presents a window into the previously undescribed transcriptome of *Plasmodium* upon host hepatocyte infection to enable a comprehensive view of the parasite's LS. These findings also provide a blueprint for future studies that extend hypotheses concerning LS gene function in *P. berghei* to human-infective *Plasmodium* parasites.

IMPORTANCE

The LS of *Plasmodium* infection is an asymptomatic yet necessary stage for producing blood-infective parasites, the causative agents of malaria. Blocking the liver stage of the life cycle

47 can prevent clinical malaria, but relatively less is known about the parasite's biology at this stage.
48 Using the rodent model *P. berghei,* we investigated whole-transcriptome changes occurring as
49 early as 2 hpi of hepatocytes. The transcriptional profiles of early time points (2, 4, 12, and 18 hpi)
50 have not been accessible before due to the technical challenges associated with liver-stage
51 infections. Our data now provides insights into these early parasite fluxes that may facilitate
52 establishment of infection, transformation and replication in the liver.
53

54 **INTRODUCTION**

55 *Plasmodium* spp., the causative agents of malaria, are eukaryotic parasites with a largely
56 conserved and complex life cycle that begins in the mammalian host by invasion of hepatocytes.
57 In these host cells, a single parasite, termed a sporozoite, will transform and then replicate
58 asexually to form thousands of merozoites, or blood-infective forms (1). After maturation and
59 release from the liver, parasites replicate within erythrocytes causing the clinical manifestation of
60 malaria. Some parasites differentiate into sexual forms (gametocytes) that are ingested by an
61 *Anopheles* mosquito during a blood meal. In the mosquito, female and male gametocytes undergo
62 sexual reproduction, and a series of developmental changes lead to a transformation into
63 sporozoites. Inoculation of these sporozoites in the host via a mosquito bite perpetuates the life
64 cycle (2). Despite the significant global burden of malaria (3), our molecular understanding of the
65 *Plasmodium* life cycle is incomplete, hindering our ability to target these parasites to prevent
66 disease and reduce transmission. In particular, the changes that enable sporozoites to transform
67 and then develop within hepatocytes are largely unknown.
68

Transcriptomic studies have been instrumental in revealing gene expression variation that accompanies stage transitions and developmental processes in *Plasmodium*. Subsequent analyses of these data have also identified transcription factors that are critical for controlling parasite progression at various stages (reviewed in (4)). Yet, only a handful of transcriptome analyses have been completed in the LS relative to other parasite forms, likely owing to the technical challenges associated with studying this stage. Still, these studies have provided important insight into LS-specific biological processes (5), including hypnozoite markers (6, 7), through comparative gene expression analysis with other stages (8), even at single-cell resolution (9). These studies examined gene expression upon the establishment of a LS-trophozoite (24 hours post-infection and thereafter); however, the early stages of LS infection (0–24 hours post-infection) for any *Plasmodium* species remains unresolved.

Our current understanding of the early stages of LS development comes from ultrastructural (10) and immunofluorescence (11) studies. Upon traversal and invasion of hepatocytes, rod-shaped sporozoites expulse unnecessary organelles into the parasitophorous vacuole (PV), which is accompanied by the formation of a protrusion, a bulbous expansion and a transformation into a spherical, replication-competent trophozoite (10). Although this metamorphosis is obvious at the cellular level, the molecular events underpinning this sequence of events remain obscure. Previous studies have examined the gene expression of sporozoites grown axenically since sporozoites can complete this transformation extracellularly if activated by BSA, calcium, and a temperature shift (12, 13). Yet, axenically-grown sporozoites show reduced viability and poor developmental capacity compared to intracellular parasites, suggesting an important role of host pathways in this process. Indeed, a recent study showed that activation of the host GPCR CXCR-4 is necessary for proper parasite metamorphosis (11), highlighting the

need to study parasite transformation, and all its subsequent development, in the context of the host cell.

Here, we present a transcriptomic survey of the early and mid-liver stages of *P. berghei* infecting human hepatoma cells. The rodent *P. berghei* and *P. yoelii* LS models are routinely used to study this stage due to their genetic accessibility and tractability relative to human-infective counterparts. Our dataset includes seven timepoints, from 2 to 48 hours post-infection (hpi), making it the most comprehensive transcriptomic analysis of the *Plasmodium* LS to date. We describe changes in gene expression associated with the early stages of *Plasmodium* intracellular development in the LS and show that upregulation of most genes important for exo-erythrocytic form (EEF) maturation occurs as early as 12 hpi. This finding suggests genes important for late-LS development are subject to dynamic expression or translational repression until protein expression is necessary. Furthermore, using co-expression analysis we identified functionally enriched gene clusters with distinct expression patterns and discovered dozens of potential regulatory DNA motifs associated with these genes. Overall, our work completes the life cycle of this important model organism, *P. berghei,* from the transcriptomic perspective, providing a resource for exploring stage-specific expression of genes, and thus providing insight into *Plasmodium* biology.

RESULTS

RNA-Seq of Early- and Mid-*P. berghei* Liver Stages. During the course of the LS, sporozoites undergo morphological changes and rapid replication. To investigate differentially expressed transcripts that flux during this stage, HuH7 or HepG2 hepatoma cells were infected with GFP-expressing *P. berghei* ANKA sporozoites. At various times post-infection, samples were

harvested, and 1000–3000 *P. berghei*-infected cells were collected by FACS (**Figure 1A**). A poor understanding exists for the early- and mid-LS, therefore greater sampling was acquired before 24 hpi at 2, 4, 12 and 18 hpi (early). Previously analyzed mid-LS samples at 24 and 48 hpi were collected to enable comparison to other studies, as well as 36 hpi, which has not been previously evaluated. *Plasmodium* infection in liver cells is highly heterogenous, with ~ 50% of sporozoites that invade liver cells failing to establish productive infections (14, 15). We ensured selection of populations enriched for productive infections within viable host cells by isolating cells that are both infected and have an uncompromised membrane (GFP^+ Sytox $Blue^-$). FACS analysis indicates that the population of infected cells (GFP-positive) shifts as a function of time, consistent with proper intrahepatic parasite maturation (**Figure 1B**). Further, our gating excluded unviable host cells (Sytox Blue-postive). In our method, we sorted directly into lysis buffer. RNA was then extracted in each sample using the Clontech kit for ultra-low input RNA. Samples were evaluated for concentration and quality using a Qubit and Bioanalyzer, respectively, and analyzed by RNA-seq if they met quality controls. To facilitate robust analysis, sample collection continued until a minimal of 3 replicates per time point were acquired, which yielded a final range of 3–8 replicates.

All samples were aligned to *H. sapiens* and *P. berghei* for analysis. As parasite nuclear division does not occur until mid-LS, <4% of the reads mapped to *P. berghei* before 24 hpi. This percentage rises continuously during mid-LS, when the parasite undergoes nuclear division and by 48 hpi ~45 % of the reads correspond to *P. berghei* (**Figure 1C**). In this report, we are focused on parasite processes that control development within hepatocytes, thus principal component analysis (PCA) was completed on *P. berghei* data after removal of batch effects. PCA revealed no major differences between the parasite transcriptomes obtained by infecting HepG2 or Huh7 cells (**Figure S1A**), but a general clustering of replicates by genotype (timepoint) was observed (**Figure**

138 **S1B**). Of note, PCA showed strong separation of 4 hpi and 2 hpi, with the latter grouping well with
139 sporozoites, highlighting the parasite transformations that must occur during these 2 hours.

140 To analyze our dataset in the context of the entire *Plasmodium* life cycle, we calculated
141 Spearman correlations on our data as well as previously published *Plasmodium* transcriptomic data
142 from sporozoites, the asexual blood stage (ABS), gametocytes, ookinetes, hypnozoites and the LS
143 (**Table S1**). This analysis spanned data obtained from *P. berghei*, *P. yoelii*, *P. cynomolgi, P. vivax*
144 and *P. falciparum*. Consistent with previous reports, the LS was more similar to the asexual blood
145 stage (ABS) than to gametocytes and ookinetes (8). Indeed, we observe two general groups
146 comprising of 1) mostly metabolically active, intracellular stages (LS, ABS), and 2) mostly motile,
147 extracellular stages (**Figure 2**). Notably, early liver stages of *P. berghei* and (axenic) *P. vivax*
148 (LS_2h/4h) fell into the latter group, being more highly correlated to sporozoites, ookinetes and
149 gametocytes than to other LS time points.

150

151 **Early Liver-Stage Transcriptome of *P. berghei*.** Thousands of statistically significant
152 differentially expressed transcripts were detected at early LS time points, with most of these
153 transcripts being downregulated at 2 and 4 hpi, and then upregulated at 12 hpi with respect to
154 sporozoites (**Figure 3A and B, Data S1**). This shift suggests a change from gene suppression to
155 activation as the parasite exits the early stage of intrahepatic development. As expected, genes
156 important for host cell traversal and invasion, such as *CELTOS*, *SUB2*, and *CSP,* were
157 downregulated at 2 hpi, concurrent with upregulation of genes important for nutrient acquisition
158 (*ZIP1, TPT, NT1*), reflecting the establishment of the infection in the host cell. Unsurprisingly, at
159 these early stages, we also observe strong upregulation of *EXP2* and *PV2*, which encode PVM-
160 associated proteins, together with several predicted exported proteins with unknown function,

indicating that early (<4 hpi) establishment and remodeling of the PVM is essential for parasite LS maturation. Interestingly, we observe that *LYTB* (IspH), the last enzyme in the isoprenoid biosynthesis pathway in the apicoplast, is among the most upregulated genes at both 2 and 4 hpi (**Table S2**). Apicoplast pathways are important potential drug targets for the development of LS antimalarials, but are not known to be involved in early-LS processes.

Translational regulation of *Plasmodium* transcripts has been extensively documented and it is known to play a pivotal role during developmental transitions in the life cycle. We found pervasive upregulation of most of the functionally characterized translational regulators in *Plasmodium*, at the exclusion of *PUF1* and *PUF2*, which appeared to be dramatically downregulated when compared to their high expression in sporozoites. *DOZI*, *ALBA1*, *ALBA2* and *ALBA4* were upregulated as early as 4 hpi (Log2FC < 2, $q < 0.01$) (**Figure S2**). Moreover, among the highest differentially expressed transcripts at 2 and 4 hpi, there was an enrichment of genes involved in RNA-protein complexes and interactions, such as *SR1*, *NOP10*, *CBF5*, *RPS12*, *NAPL* (**Table S3**). Thus, translational regulation likely plays an important role in the early stages of *Plasmodium* infection of the liver.

At ~24 hpi and thereafter, the single-nucleated trophozoites replicate and subsequently mature into LS schizonts, each harboring tens of thousands of nuclei. Previous work examining the LS stage transcriptome at these mid-stages identified hundreds of differentially expressed genes involved in translation, metabolism, protein trafficking and redox processes (5, 8). Since we saw a strong correlation between 12 hpi and mid-liver stages (Spearman correlation = 0.837—0.949, **Figure 2**), we questioned how early a statistically significant upregulation of the core mid-LS transcriptome could be observed in our dataset. We found 1,197 genes in our dataset that are significantly upregulated at 24, 36 and 48 hpi compared to sporozoites ($q < 0.01$), constituting

about 20% of the *P. berghei* genome (**Figure 3A** and **B**). Interestingly, we find that 87% of transcripts that are upregulated throughout the mid-liver stages (24 hpi through 48 hpi) are upregulated as early as 12 hpi (**Figure 3C**). More specifically, 50% of the genes that are upregulated in the mid-liver stages are first observed to be upregulated at 12 hpi (**Figure 3D**).

Co-Expression Analysis Identifies Functionally Enriched Gene Clusters. To identify co-expression patterns that may inform future functional studies, we performed a clustering analysis of the k-means for all differentially expressed genes for all of the samples included in our dataset. Fourteen clusters emerged from this hierarchical clustering analysis (**Figure 4A, Data S2**). These clusters could be further grouped within three major co-expression patterns when columns were grouped by sample genotype (timepoint). The first major cluster group (clusters 3, 11 and 13) includes genes that are upregulated early during infection (spz, 2 and 4 hpi) and are generally downregulated throughout the rest of LS infection, such as *ETRAMP*s and *SPELD*. The second major cluster group (clusters 1, 2, 4, 7, 8, 9, 12, and 14) includes genes that are downregulated during the early stages of infection, but are then consistently upregulated from 24 to 48 hpi. The third major cluster group (clusters 5, 6, and 10) includes genes that are upregulated throughout the entire LS.

To investigate possible enrichment of biological processes of co-expressed genes, we analyzed each cluster by gene ontology (GO). Such analyses revealed the enrichment of various GO terms for each of the clusters ($p < 0.01$). We prioritized clusters for which at least one GO term was enriched by a *p-adj* (Bonferroni) < 0.01. Cluster 3 stood out as highly enriched despite 142 out of the total 248 genes in this cluster not being annotated. For this cluster, enrichment analysis indicated significant enrichment of “interspecies interaction” (GO:0044419, $p < 1.91E-$

07) as well as locomotion (GO:0040011, $p < 0.0005679$) and signal transduction (GO:0007165, $p < 0.00049572$) (**Figure 4B**). Genes in this cluster are highly expressed in sporozoites, and thus appear to be strongly downregulated during infection (**Figure 4C**). In agreement with this result, this cluster includes genes that have been previously shown to play an important role during invasion (*CELTOS*, *SPECT1*, *TRAP*), interactions with the host liver cell (*UIS3, UIS4, CSP, p36, p52*), and translational control of liver-stage specific transcripts (*UIS2, PUF1, PUF2*) (16).

Cluster 14 was enriched for "oxidation-reduction process" (GO:0055114, $p < 9.01E-05$), "DNA replication" (GO:0006260, $p < 0.00164223$), and "intracellular protein transport" (GO:0006886, $p < 0.00941436$) (**Figure 4B**). In this group, genes involved in redox-regulatory processes (*FNR, TRX-PX2*), as well as biosynthetic genes such as *G3PDH*, can be found. Expression of genes under the redox group appears to peak by ~12 hpi and then remains stably upregulated throughout infection. This expression pattern highlights the need for this machinery to mitigate potential stress due to the dramatic parasite replication and growth that is initiated at ~24 hpi (**Figure 4C**). Little is known about redox biology in *Plasmodium* parasites, particularly during the LS, but these processes have historically been key pathways for drug discovery. Indeed, atovaquone, a drug for malaria prophylaxis in combination with proguanil, inhibits liver stage parasites in vitro by impairing mitochondrial redox metabolism via targeting the cytochrome bc_1 complex (17). This dataset may serve as a starting point to discover more LS targets involved in redox metabolism. Furthermore, although not enriched in our GO analysis, we observed that several important liver-specific genes are found in this cluster, such as *IBIS1*, *LISP1*, and *LISP2*. Finally, in cluster 6, we saw enrichment of core functions such as "gene expression" (GO:0010467, $p < 5.71E-05$) and "RNA processing" (GO:0006396, $p < 5.98E-06$), which contains 656 genes. As expected of housekeeping functions, these genes appear to be expressed throughout LS infection.

Our analysis identified several clusters with enriched GO terms, some which accurately describe the known LS biology at different timepoints. Although GO enrichment provided a useful assessment of differentially expressed processes, we note that it is limited in its reach in *Plasmodium* when compared to other model organisms since ~40% of the genome remains unannotated. Hence, to further explore the composition of these co-expression clusters, we made use of the Rodent Malaria genetically modified parasite database (RMgmDB) to provide phenotypic information about our clusters throughout the life cycle (18). Interestingly, we observe that while most clusters have a high proportion of genes for which disruption resulted in phenotypes across the entire life cycle, only a few clusters had genes that displayed phenotypes exclusively in sporozoite and/or liver stage (**Figure S3**). Specifically, clusters 3 and 14 had the highest percentage of spz/LS-specific genes (13 and 9%, respectively), reinforcing the potential for identifying new LS drug and vaccine targets within these clusters.

Expression Dynamics of AP2 Transcription Factors. Transcriptional regulation of gene expression has been extensively studied in the intraerythrocytic developmental cycle (IDC) and mosquito stages of *P. berghei* and *P. falciparum*. The AP2 transcription factors (TFs), comprised of 26 genes in *P. berghei*, are the best-characterized family of TFs in apicomplexans (**Figure 5A**). AP2s are known to regulate *Plasmodium* transitions into different developmental stages and have emerged as key factors leading to both sexual commitment and sex differentiation (reviewed in (4)). Unsurprisingly, we observe that AP2 genes with established functions in mosquito stages (*AP2-O*, *AP2-O2*) and those involved in sporozoite development (*AP2-SPs*) are downregulated throughout the liver stages (**Figure 5A**). The only ApiAP2 TF known to play a role in LS development is *AP2-L*. *AP2-L* (-/-) parasites are able to traverse and invade liver cells, but arrest

in the schizont stage (19). *AP2-L* transcripts are abundant in sporozoites and thus appear to be strongly downregulated during infection, as early as 2 hpi (**Figure 5A**).

We observe strong upregulation (~3-fold) of *AP2-G2* at 2 and 4 hpi. AP2-G2 has been shown to act as a repressor during the BS and gametocyte development, and to have different targets during these stages (20, 21). A group of such targets corresponds to the liver-specific genes *LISP1* and *TREP*, which are important for LS schizont maturation and expressed during late LS infection (21). Interestingly, we observe that *AP2-G2* expression is negatively correlated to the average expression of the main clusters harboring this set of genes, including clusters 1, 9 and 14 (**Data S3**). Thus, it is plausible that during the first hours of infection, *AP2-G2* acts as a repressor of genes involved in later stages of LS development, many of which remain uncharacterized.

Interestingly, we observed significant upregulation of the uncharacterized ApiAP2s PBANKA_0835200 and PBANKA_0109500 throughout the LS starting at 12 hpi, in contrast to the early upregulation of *AP2-G2*. While still functionally uncharacterized, their orthologs in *P. falciparum* have been recently shown to co-express during differentiation in gametocytogenesis, and to be inversely correlated to genes involved in ABS development. This expression pattern suggests they may have a role as co-repressors of genes involved in the ABS (22). In our dataset, we observe a strong correlation with clusters 11, 12 (both negative) and cluster 8 (positive).

We sought to identify enriched DNA motifs in each of the co-expression clusters by analyzing the 5' UTR sequences (1 kb) of their genes against the upstream sequence for all of the genes in other clusters using DREME (**Data S3**) (23). While genes in clusters 1, 2, 5 and 13 lacked any enriched DNA motifs, *de novo* discovery uncovered hundreds of DNA motifs in the remaining clusters, with the topmost enriched motif shown in **Figure 5B**. We found that the most significant motif in cluster 12 (T[G/C]TAACA) matched the motif recognized by ApiAP2

276 PBANKA_0521700 (GTGTTACAC, $p < 1.28e-05$). This cluster included genes that are mostly
277 downregulated throughout the LS until the later time points in our time series, such as the BS
278 schizont-specific genes *SERA2* and *SERA3*. Additionally, PBANKA_0521700 expression was
279 strongly correlated to cluster 12 ($r = 0.83$, $p < 0.021$), suggesting this cluster might harbor
280 previously unknown targets of this ApiAP2 (**Figure 5B**).
281
282 **DISCUSSION**
283 Our data provide novel insights into gene expression fluxes throughout *Plasmodium*
284 development within hepatocytes. The transcriptional blueprints provided by our time series
285 enables comparison of early-, mid- and late-liver stage parasite processes for the first time. We
286 found 146 genes exclusively upregulated early, such as *EIF5*; and 482 genes, including *SERA1*
287 and *LISP2,* exclusively upregulated in the mid-liver stages (**Figure S4**). Furthermore, our datasets
288 recapitulated well-established gene expression patterns of key LS genes, and overall were largely
289 in agreement with recently reported datasets, supporting the validity of our approach. Through our
290 analysis, we identified a key shift in parasite gene expression that occurs at 12 hpi, and the role of
291 transcription factors in driving LS maturation. Specifically, we explored potential transcriptional
292 regulation of co-expressing genes by analyzing their upstream sequences for enrichment of
293 potential DNA binding motifs, and their correlation to *P. berghei* AP2 transcription factors. Our
294 results revealed an association between the uncharacterized PBANKA_0521700 AP2 TF and
295 cluster 12. PBANKA_0521700 is preferentially expressed in the ring stages of the IDC and is
296 refractory to disruption in the BS (24, 25), hampering functional studies of this gene. Our data, in
297 conjunction with previously reported *P. berghei* RNA-seq (8, 24–26) and single cell studies

298 covering the entire life cycle (9), could be useful to refine hypotheses about the functions and
299 targets of this TF as well as other AP2 TFs.

300 While AP2 TFs have been at the center of gene expression studies in *Plasmodium*, novel
301 "omics" approaches have begun uncovering other layers of gene regulation. Indeed, post-
302 transcriptional regulation, such as N^6-methyladenosine (m^6A) of mRNA and alternative splicing,
303 have recently been recognized as essential for fine-tuning gene expression in blood and sexual
304 stages (27, 28). In particular, disruption of the splicing factor *Pb*SR-MG was shown to perturb sex-
305 specific alternative splicing, thus demonstrating its role as a cellular differentiation regulator (29).
306 Interestingly, we observed a dramatic upregulation of the splicing factor SR1 coinciding with the
307 parasite's metamorphoses in the LS, hinting at an important role for alternative splicing during this
308 stage. Future reverse genetic studies may help establish a role for alternative splicing in the LS.

309 A well-documented form of gene expression regulation in *Plasmodium* occurs at the
310 translational level. Translational repression (TR) of hundreds of transcripts has been reported at
311 most stages of the *P. berghei* life cycle (30). TR is particularly pervasive in the sporozoite
312 transition from the mosquito to the mammalian host (31, 32). During this transition, hundreds of
313 transcripts that are highly expressed in sporozoites are stored in mRNA granules, until infection
314 of the host relieves this repression resulting in protein translation. The extent to which a TR
315 program operates in the LS is currently unknown. However, we observed that ~50% of all
316 transcripts upregulated after 24 hpi are also upregulated at 12 hpi, including some with known
317 roles in LS schizont maturation (*IBIS1* and *BP2*). Furthermore, we see upregulation of several
318 known translation regulators *DOZI, ALBA1,-2,-4*, which could potentially repress translation of
319 transcripts important for late LS development and/or the subsequent transition to the ABS.
320 Unfortunately, this possibility will be exceedingly difficult to test in the absence of robust global

proteomic analysis of the early LS parasite. Nonetheless, our data, coupled with recent RNA-seq and proteomic studies of the more accessible late LS, can provide a starting point to address this question (8, 33).

Previous work examining the transcriptional changes of axenically grown early LS *P. vivax* identified upregulation of calcium-related proteins (RACK1) and RNA-binding proteins (*ALBA1*, *-2* and *-4*) (34) . We saw upregulation of the *P. berghei* orthologs of these genes as well as hundreds of other genes, dramatically expanding the dataset for genes upregulated at this stage (**Figure S5**). For example, we found *LYTB* is upregulated at 2 and 4 hpi, indicating isoprenoids may be important at this time. While the FASII and *de novo* heme biosynthesis pathways have been genetically and chemically validated as essential to the late liver stages, less is known about isoprenoid biosynthesis during the early liver stages (35, 36). When intracellular sporozoites metamorphosize to replication-competent trophozoites, most organelles are expelled at the exclusion of the nucleus, mitochondrion, and apicoplast (10). Thus, it is plausible that the apicoplast serves an important metabolic role with isoprenoids in the liver stages of infection. Unfortunately, the use of isoprenoid biosynthesis inhibitors has yielded inconclusive results about its function during the LS (37, 38), emphasizing the need for future genetic studies to elucidate the role of isoprenoid biosynthesis throughout intrahepatic development. Thus, we anticipate our data will be useful to guide future reverse genetic and functional studies to investigate the role of *Plasmodium* genes with important early- and mid-LS functions.

Our understanding of *Plasmodium* LS biology still lags behind that of other parasite life cycle stages, hindering the development of much-needed prophylactic measures to combat malaria. Our work represents a window into the previously undescribed transcriptome of the early LS upon host cell infection and offers a comprehensive view of the *Plasmodium* LS. Future studies

344 expanding on our analysis and validating time-specific LS genes will further advance our
345 molecular understanding of this critical step in the *Plasmodium* life cycle.
346
347 **MATERIALS AND METHODS**
348
349 **Parasites.** Sporozoites were freshly harvested prior to experiments from dissected salivary glands
350 of *Anopheles stephensi* mosquitoes infected with *P. berghei* ANKA stably expressing a green
351 fluorescent protein (GFP) purchased from the New York University Langone Medical Center
352 Insectary.
353
354 **Cell culture.** HepG2 were purchased from ATCC and HuH7 cells were a kind gift from Dr. Peter
355 Sorger (Harvard Medical School). Hepatocytes used for *P. berghei* infections were maintained in
356 Dulbecco's Modified Eagle Medium (DMEM) with L-glutamine (Gibco) supplemented with 10%
357 heat-inactivated fetal bovine serum (HI-FBS) (v/v) (Sigma-Aldrich) and 1% antibiotic-
358 antimycotic (Thermo Fisher Scientific) in a standard tissue culture incubator (37°C, 5% CO_2).
359
360 **Sample collection for RNA-seq.** Infected hepatoma cells were collected as previously described
361 (39). Briefly, T25 flasks were seeded with $3x10^5$ HepG2 or $8x10^4$ HuH7 cells. About 24 hours
362 after seeding, cells were infected with $1x10^5$ GFP-expressing *P. berghei*-ANKA sporozoites.
363 Infected cells and uninfected controls were sorted directly into RNA lysis buffer (Clontech) using
364 the BD FACSAria II cell sorter (BD Biosciences) at the Duke Human Vaccine Institute. Sytox
365 blue was used as a live/dead cell indicator (Thermo Fisher Scientific). Infected cells were collected
366 by sorting of the GFP, and gated compared to uninfected hepatoma cells. RNA was extracted using

SMART-seq v4 Ultra Low Input RNA Kit for Sequencing (Clonetech) and libraries were prepared at the Duke Next Generation Sequencing Core Facility and sequenced on the Illumina HiSeq 4000 as 50 base pair single-end reads. Samples (4–5) were pooled on each flow cell lane.

RNA-seq and differential expression analysis. RNA-seq data were processed using the TrimGalore toolkit (40) which employs Cutadapt (41) to trim low-quality bases and Illumina sequencing adapters from the 3' end of the reads. Only reads that were 20 nt or longer after trimming were kept for further analysis. Reads were mapped to a combination of the GRCh37v75 (42) version of the human genome and the PbANKAv3 of the *P. berghei* genome using the STAR RNA-seq alignment tool (43). Reads were kept for subsequent analysis if they mapped to a single genomic location. All samples mapping >1 million reads to the *P. berghei* genome were used for a preliminary analysis. Gene counts were compiled using the HTSeq tool (44). Only *P. berghei* genes that had at least 10 reads in any given library were used in subsequent analysis. Normalization and differential expression were carried out using the DESeq2 (45) Bioconductor (46) package with the R statistical programming environment (47). The false discovery rate was calculated to control for multiple hypothesis testing. When calculating the differential expression between genes at each time point relative to the control, the cell type and sequencing batch were included as cofactors in the model.

Spearman correlations between published *P. berghei* RNA-seq datasets and our own were calculated and plotted using the *cor* function in the *stats* R package.

Clustering analysis. To determine the different patterns of gene expression across all groups of samples, we first identified genes that showed differential expression in at least one of the

comparisons performed (FDR <= 5%). The genes were the clustered across all samples by a correlation distance using complete linkage after z-score transformation. The *NbClust* (48) package was used to separate the gene expression across all samples into distinct clusters.

De novo motif discovery was performed using DREME from the MEME suite (23). For each cluster the input data set was the upstream 1000 kb region of each gene within that cluster, and the negative set was the upstream region of genes that were not in that cluster. The analysis was run in discriminative mode, scanning the given strand only, with the predicted motif size of 4–10 bp and cut-off E value of 0.05. The top most enriched motif for each cluster was then analyzed with TOMTOM (49) to compare to previously *in silico* discovered motifs (50).

The correlation matrix was generated in PRISM by calculating the Pearson correlation between each AP2 transcription factor and the average fold change expression for all the genes in each cluster.

Gene Ontology (GO). GO analyses for each cluster were performed using the GO enrichment tool of Biological Processes in PlasmoDB (51) with a cutoff of $p < 0.01$. The number of genes from the cluster in each of the representative top-scoring GO terms (lowest *p*-values) were plotted.

ACKNOWLEDGEMENTS

This work is funded by the NIH (DP2AI138239, to E.R.D), the CM Hauser Fellowship (M.T.M), and the NSF (DGE-1644868, to K.S.). The content of this study is solely the responsibility of the authors and does not necessarily represent the official views of the NIH.

We thank Prof. Ana Rodriguez and Sandra Gonzalez from the NYU Insectary for providing *Plasmodium*-infected mosquitoes, David Corcoran from the Duke Genomic Analysis and

Bioinformatics (GCB) Core Facility, the DHVI Flow Cytometry Core Facility, and Joseph Saelens. We also thank Prof. Photini Sinnis, Amanda Balaban, and the JHMRI Insectary and Parasitology Core Facilities for their help. We thank Luisa Toro Moreno for data managing support, and Profs. Jen-Tsan Ashley Chi and Steven Haase for useful discussions.

Author contributions

Conception or design of the work— M.T-M, K.S, D.P, E.R.D

Data collection—K.S, D.P, E.R.D

Data analysis and interpretation— M.T-M, K.S, T.S

Drafting the article— M.T-M

Critical revision and contributions to the article— K.S, E.R.D

Final approval of the version to be published— M.T-M, K.S, T.S, D.P, E.R.D

REFERENCES

1. Prudêncio M, Rodriguez A, Mota MM. 2006. The silent path to thousands of merozoites: the Plasmodium liver stage. Nat Rev Microbiol 4:849–856.
2. Aly ASI, Vaughan AM, Kappe SHI. 2009. Malaria Parasite Development in the Mosquito and Infection of the Mammalian Host. Annu Rev Microbiol 63:195–221.
3. World Health Organization. 2019. World Malaria Report.
4. Josling GA, Williamson KC, Llinás M. 2018. Regulation of Sexual Commitment and Gametocytogenesis in Malaria Parasites. Annu Rev Microbiol 72:501–519.
5. Tarun AS, Peng X, Dumpit RF, Ogata Y, Silva-Rivera H, Camargo N, Daly TM, Bergman

LW, Kappe SHI. 2008. A combined transcriptome and proteome survey of malaria parasite liver stages. Proc Natl Acad Sci U S A 105:305–10.

6. Bertschi NL, Voorberg-Van der Wel A, Zeeman AM, Schuierer S, Nigsch F, Carbone W, Knehr J, Gupta DK, Hofman SO, van der Werff N, Nieuwenhuis I, Klooster E, Faber BW, Flannery EL, Mikolajczak SA, Chuenchob V, Shrestha B, Beibel M, Bouwmeester T, Kangwanrangsan N, Sattabongkot J, Diagana TT, Kocken CHM, Roma G. 2018. Transcriptomic analysis reveals reduced transcriptional activity in the malaria parasite Plasmodium cynomolgi during progression into dormancy. Elife 7:e41081.

7. Cubi R, Vembar SS, Biton A, Franetich JF, Bordessoulles M, Sossau D, Zanghi G, Bosson-Vanga H, Benard M, Moreno A, Dereuddre-Bosquet N, Le Grand R, Scherf A, Mazier D. 2017. Laser capture microdissection enables transcriptomic analysis of dividing and quiescent liver stages of Plasmodium relapsing species. Cell Microbiol 19:e12735.

8. Caldelari R, Dogga S, Schmid MW, Franke-Fayard B, Janse CJ, Soldati-Favre D, Heussler V. 2019. Transcriptome analysis of Plasmodium berghei during exo-erythrocytic development. Malar J 18.

9. Howick VM, Russell AJC, Andrews T, Heaton H, Reid AJ, Natarajan K, Butungi H, Metcalf T, Verzier LH, Rayner JC, Berriman M, Herren JK, Billker O, Hemberg M, Talman AM, Lawniczak MKN. 2019. The Malaria Cell Atlas: Single parasite transcriptomes across the complete Plasmodium life cycle. Science (80-) 365:eaaw2619.

10. Jayabalasingham B, Bano N, Coppens I. 2010. Metamorphosis of the malaria parasite in the liver is associated with organelle clearance. Cell Res 20:1043–1059.

11. Bando H, Pradipta A, Iwanaga S, Okamoto T, Okuzaki D, Tanaka S, Vega-Rodríguez J, Lee Y, Ma JS, Sakaguchi N, Soga A, Fukumoto S, Sasai M, Matsuura Y, Yuda M, Jacobs-

459 Lorena M, Yamamoto M. 2019. CXCR4 regulates Plasmodium development in mouse and
460 human hepatocytes. J Exp Med 216:1733–1748.
461 12. Kaiser K, Camargo N, Kappe SHI. 2003. Transformation of sporozoites into early
462 exoerythrocytic malaria parasites does not require host cells. J Exp Med 197:1045–1050.
463 13. Doi Y, Shinzawa N, Fukumoto S, Okano H, Kanuka H. 2011. Calcium signal regulates
464 temperature-dependent transformation of sporozoites in malaria parasite development. Exp
465 Parasitol 128:176–180.
466 14. Prudêncio M, Rodrigues CD, Ataíde R, Mota MM. 2008. Dissecting in vitro host cell
467 infection by Plasmodium sporozoites using flow cytometry. Cell Microbiol 10:218–224.
468 15. Risco-Castillo V, Topçu S, Marinach C, Manzoni G, Bigorgne AE, Briquet S, Baudin X,
469 Lebrun M, Dubremetz J-F, Silvie O, Amino R, Giovannini D, Thiberge S, Gueirard P,
470 Boisson B, Dubremetz J-F, Prévost M-C, Ishino T, Yuda M, Ménard R, Bano N, Romano
471 JD, Jayabalasingham B, Coppens I, Besteiro S, Dubremetz JF, Lebrun M, Bhanot P,
472 Schauer K, Coppens I, Nussenzweig V, Charoenvit Y, Leef MF, Yuan LF, Sedegah M,
473 Beaudoin RL, Deligianni E, Morgan RN, Bertuccini L, Wirth CC, Monerri NCS de, Spanos
474 L, Blackman MJ, Louis C, Pradel G, Siden-Kiamos I, Dunstone MA, Tweten RK, Frevert
475 U, Engelmann S, Zougbédé S, Stange J, Ng B, Matuschewski K, Liebes L, Yee H, Garg S,
476 Agarwal S, Kumar S, Yazdani SS, Chitnis CE, Singh S, Hamon MA, Ribet D, Stavru F,
477 Cossart P, Ishino T, Yano K, Chinzei Y, Yuda M, Ishino T, Chinzei Y, Yuda M, Janse CJ,
478 Ramesar J, Waters AP, Kafsack BFC, Pena JDO, Coppens I, Ravindran S, Boothroyd JC,
479 Carruthers VB, Kaiser K, Camargo N, Coppens I, Morrisey JM, Vaidya AB, Kappe SH,
480 Kariu T, Ishino T, Yano K, Chinzei Y, Yuda M, Manzoni G, Briquet S, Risco-Castillo V,
481 Gaultier C, Topçu S, Ivănescu ML, Franetich JF, Hoareau-Coudert B, Mazier D, Silvie O,

Ménard R, Tavares J, Cockburn I, Markus M, Zavala F, Amino R, Mordue DG, Desai N, Dustin M, Sibley LD, Moreira CK, Templeton TJ, Lavazec C, Hayward RE, Hobbs CV, Kroeze H, Janse CJ, Waters AP, Sinnis P, Coppi A, Mota MM, Pradel G, Vanderberg JP, Hafalla JC, Frevert U, Nussenzweig RS, Nussenzweig V, Rodríguez A, Mota MM, Hafalla JC, Rodriguez A, Prudêncio M, Rodrigues CD, Ataíde R, Mota MM, Ramakrishnan C, Delves MJ, Lal K, Blagborough AM, Butcher G, Baker KW, Sinden RE, Risco-Castillo V, Topçu S, Son O, Briquet S, Manzoni G, Silvie O, Roiko MS, Svezhova N, Carruthers VB, Schuerch DW, Wilson-Kubalek EM, Tweten RK, Silvie O, Rubinstein E, Franetich J-F, Prenant M, Belnoue E, Rénia L, Hannoun L, Eling W, Levy S, Boucheix C, Mazier D, Silvie O, Greco C, Franetich JF, Dubart-Kupperschmitt A, Hannoun L, Gemert GJ van, Sauerwein RW, Levy S, Boucheix C, Rubinstein E, Mazier D, Silvie O, Charrin S, Billard M, Franetich JF, Clark KL, Gemert GJ van, Sauerwein RW, Dautry F, Boucheix C, Mazier D, Rubinstein E, Silvie O, Franetich JF, Boucheix C, Rubinstein E, Mazier D, Talman AM, Lacroix C, Marques SR, Blagborough AM, Carzaniga R, Ménard R, Sinden RE, Tavares J, Formaglio P, Thiberge S, Mordelet E, Rooijen N Van, Medvinsky A, Ménard R, Amino R, Tsuji M, Mattei D, Nussenzweig RS, Eichinger D, Zavala F, Wirth CC, Glushakova S, Scheuermayer M, Repnik U, Garg S, Schaack D, Kachman MM, Weißbach T, Zimmerberg J, Dandekar T, al. et, Yamauchi LM, Coppi A, Snounou G, Sinnis P, Yoshimori T, Yamamoto A, Moriyama Y, Futai M, Tashiro Y, Zhao Y, Marple AH, Ferguson DJP, Bzik DJ, Yap GS, Zuber MX, Strittmatter SM, Fishman MC. 2015. Malaria Sporozoites Traverse Host Cells within Transient Vacuoles. Cell Host Microbe 18:593–603.

16. Vaughan AM, Kappe SHI. 2017. Malaria parasite liver infection and exoerythrocytic biology. Cold Spring Harb Perspect Med 7:a025486.

505 17. Siregar JE, Kurisu G, Kobayashi T, Matsuzaki M, Sakamoto K, Mi-ichi F, Watanabe Y,
506 Hirai M, Matsuoka H, Syafruddin D, Marzuki S, Kita K. 2015. Direct evidence for the
507 atovaquone action on the Plasmodium cytochrome bc 1 complex. Parasitol Int 64:295–300.
508 18. Janse CJ, Kroeze H, van Wigcheren A, Mededovic S, Fonager J, Franke-Fayard B, Waters
509 AP, Khan SM. 2011. A genotype and phenotype database of genetically modified malaria-
510 parasites. Trends Parasitol.
511 19. Iwanaga S, Kaneko I, Kato T, Yuda M. 2012. Identification of an AP2-family Protein That
512 Is Critical for Malaria Liver Stage Development. PLoS One 7:e47557.
513 20. Yuda M, Iwanaga S, Kaneko I, Kato T. 2015. Global transcriptional repression: An initial
514 and essential step for Plasmodium sexual development. Proc Natl Acad Sci U S A
515 112:12824–12829.
516 21. Modrzynska K, Pfander C, Chappell L, Yu L, Suarez C, Dundas K, Gomes AR, Goulding
517 D, Rayner JC, Choudhary J, Billker O. 2017. A Knockout Screen of ApiAP2 Genes Reveals
518 Networks of Interacting Transcriptional Regulators Controlling the Plasmodium Life Cycle.
519 Cell Host Microbe 21:11–22.
520 22. Biljon R van, Wyk R van, Painter H, Orchard L, Reader J, Niemand J, Llinas M, Birkholtz
521 L-M. 2019. Hierarchical transcriptional control regulates Plasmodium falciparum sexual
522 differentiation. bioRxiv 633222.
523 23. Bailey TL. 2011. DREME: Motif discovery in transcription factor ChIP-seq data.
524 Bioinformatics 27:1653–1659.
525 24. Otto TD, Böhme U, Jackson AP, Hunt M, Franke-Fayard B, Hoeijmakers WAM, Religa
526 AA, Robertson L, Sanders M, Ogun SA, Cunningham D, Erhart A, Billker O, Khan SM,
527 Stunnenberg HG, Langhorne J, Holder AA, Waters AP, Newbold CI, Pain A, Berriman M,

528 Janse CJ. 2014. A comprehensive evaluation of rodent malaria parasite genomes and gene
529 expression. BMC Med 12:86.
530 25. Modrzynska K, Pfander C, Chappell L, Yu L, Suarez C, Dundas K, Gomes AR, Goulding
531 D, Rayner JC, Choudhary J, Billker O. 2017. A Knockout Screen of ApiAP2 Genes Reveals
532 Networks of Interacting Transcriptional Regulators Controlling the Plasmodium Life Cycle.
533 Cell Host Microbe 21:11–22.
534 26. LaMonte GM, Orjuela-Sanchez P, Calla J, Wang LT, Li S, Swann J, Cowell AN, Zou BY,
535 Abdel-Haleem Mohamed AM, Villa Galarce ZH, Moreno M, Tong Rios C, Vinetz JM,
536 Lewis N, Winzeler EA. 2019. Dual RNA-seq identifies human mucosal immunity protein
537 Mucin-13 as a hallmark of Plasmodium exoerythrocytic infection. Nat Commun 10:488.
538 27. Baumgarten S, Bryant JM, Sinha A, Reyser T, Preiser PR, Dedon PC, Scherf A. 2019.
539 Transcriptome-wide dynamics of extensive m6A mRNA methylation during Plasmodium
540 falciparum blood-stage development. Nat Microbiol 1–14.
541 28. Viaud J, Zeghouf M, Barelli H, Zeeh J-C, Padilla A, Guibert B, Chardin P, Royer CA,
542 Cherfils J, Chavanieu A. 2007. Structure-based discovery of an inhibitor of Arf activation
543 by Sec7 domains through targeting of protein-protein complexes. Proc Natl Acad Sci U S
544 A 104:10370–5.
545 29. Yeoh LM, Goodman CD, Mollard V, McHugh E, Lee VV, Sturm A, Cozijnsen A,
546 McFadden GI, Ralph SA. 2019. Alternative splicing is required for stage differentiation in
547 malaria parasites. Genome Biol 20:151.
548 30. Lasonder E, Rijpma SR, Van Schaijk BCL, Hoeijmakers WAM, Kensche PR, Gresnigt MS,
549 Italiaander A, Vos MW, Woestenenk R, Bousema T, Mair GR, Khan SM, Janse CJ, Bártfai
550 R, Sauerwein RW. 2016. Integrated transcriptomic and proteomic analyses of P. Falciparum

551 gametocytes: Molecular insight into sex-specific processes and translational repression.
552 Nucleic Acids Res 44:6087–6101.
553 31. Muller I, Jex AR, Kappe SHI, Mikolajczak SA, Sattabongkot J, Patrapuvich R, Lindner S,
554 Flannery EL, Koepfli C, Ansell B, Lerch A, Emery-Corbin SJ, Charnaud S, Smith J,
555 Merrienne N, Swearingen KE, Moritz RL, Petter M, Duffy MF, Chuenchob V. 2019.
556 Transcriptome and histone epigenome of Plasmodium vivax salivary-gland sporozoites
557 point to tight regulatory control and mechanisms for liver-stage differentiation in relapsing
558 malaria. Int J Parasitol 49:501–513.
559 32. Lindner SE, Swearingen KE, Shears MJ, Walker MP, Vrana EN, Hart KJ, Minns AM,
560 Sinnis P, Moritz RL, Kappe SHI. 2019. Transcriptomics and proteomics reveal two waves
561 of translational repression during the maturation of malaria parasite sporozoites. Nat
562 Commun 10:4964.
563 33. Shears MJ, Sekhar Nirujogi R, Swearingen KE, Renuse S, Mishra S, Jaipal Reddy P, Moritz
564 RL, Pandey A, Sinnis P. 2019. Proteomic Analysis of Plasmodium Merosomes: The Link
565 between Liver and Blood Stages in Malaria. J Proteome Res 18:3404–3418.
566 34. Roth A, Adapa SR, Zhang M, Liao X, Saxena V, Goffe R, Li S, Ubalee R, Saggu GS, Pala
567 ZR, Garg S, Davidson S, Jiang RHY, Adams JH. 2018. Unraveling the Plasmodium vivax
568 sporozoite transcriptional journey from mosquito vector to human host. Sci Rep 8:12183.
569 35. Nagaraj VA, Sundaram B, Varadarajan NM, Subramani PA, Kalappa DM, Ghosh SK,
570 Padmanaban G. 2013. Malaria parasite-synthesized heme is essential in the mosquito and
571 liver stages and complements host heme in the blood stages of infection. PLoS Pathog
572 9:e1003522.
573 36. Rizopoulos Z, Matuschewski K, Haussig JM. 2016. Distinct prominent roles for enzymes

574 of Plasmodium berghei heme biosynthesis in sporozoite and liver stage maturation. Infect
575 Immun 84:3252–3262.
576 37. Baumeister S, Wiesner J, Reichenberg A, Hintz M, Bietz S, Harb OS, Roos DS, Kordes M,
577 Friesen J, Matuschewski K, Lingelbach K, Jomaa H, Seeber F. 2011. Fosmidomycin uptake
578 into Plasmodium and Babesia-infected erythrocytes is facilitated by parasite-induced new
579 permeability pathways. PLoS One 6:e19334.
580 38. Nair SC, Brooks CF, Goodman CD, Strurm A, McFadden GI, Sundriyal S, Anglin JL, Song
581 Y, Moreno SNJ, Striepen B. 2011. Apicoplast isoprenoid precursor synthesis and the
582 molecular basis of fosmidomycin resistance in Toxoplasma gondii. J Exp Med 208:1547–
583 1559.
584 39. Posfai D, Sylvester K, Reddy A, Ganley JG, Wirth J, Cullen QE, Dave T, Kato N, Dave SS,
585 Derbyshire ER. 2018. Plasmodium parasite exploits host aquaporin-3 during liver stage
586 malaria infection. PLOS Pathog 14:e1007057.
587 40. Krueger F. 2017. Babraham Bioinformatics - Trim Galore! Version 044.
588 41. Martin M. 2011. Cutadapt removes adapter sequences from high-throughput sequencing
589 reads. EMBnet.journal 17:10.
590 42. Kersey PJ, Staines DM, Lawson D, Kulesha E, Derwent P, Humphrey JC, Hughes DST,
591 Keenan S, Kerhornou A, Koscielny G, Langridge N, McDowall MD, Megy K, Maheswari
592 U, Nuhn M, Paulini M, Pedro H, Toneva I, Wilson D, Yates A, Birney E. 2012. Ensembl
593 Genomes: An integrative resource for genome-scale data from non-vertebrate species.
594 Nucleic Acids Res 40:D91-7.
595 43. Dobin A, Davis CA, Schlesinger F, Drenkow J, Zaleski C, Jha S, Batut P, Chaisson M,
596 Gingeras TR. 2013. STAR: Ultrafast universal RNA-seq aligner. Bioinformatics 29:15–21.

44. Anders S. 2010. HTSeq: Analysing high-throughput sequencing data with Python. … embl de/users/anders/HTSeq/doc/overview html.

45. Love MI, Huber W, Anders S. 2014. Moderated estimation of fold change and dispersion for RNA-seq data with DESeq2. Genome Biol 15:550.

46. Huber W, Carey VJ, Gentleman R, Anders S, Carlson M, Carvalho BS, Bravo HC, Davis S, Gatto L, Girke T, Gottardo R, Hahne F, Hansen KD, Irizarry RA, Lawrence M, Love MI, MaCdonald J, Obenchain V, Oleš AK, Pagès H, Reyes A, Shannon P, Smyth GK, Tenenbaum D, Waldron L, Morgan M. 2015. Orchestrating high-throughput genomic analysis with Bioconductor. Nat Methods 12:115–121.

47. The R Foundation. 2018. R: The R Project for Statistical Computing.

48. Charrad M, Ghazzali N, Boiteau V, Niknafs A. 2015. NbClust : An R Package for Determining the Relevant Number of Clusters in a Data Set. J Stat Softw 61:1–36.

49. Gupta S, Stamatoyannopoulos JA, Bailey TL, Noble W. 2007. Quantifying similarity between motifs. Genome Biol 8:R24.

50. Campbell TL, De Silva EK, Olszewski KL, Elemento O, Llinás M. 2010. Identification and genome-wide prediction of DNA binding specificities for the ApiAP2 family of regulators from the malaria parasite. PLoS Pathog 6:e1001165.

51. Collaborativea TPGD. 2001. PlasmoDB: An integrative database of the Plasmodium falciparum genome. Tools for accessing and analyzing finished and unfinished sequence data. Nucleic Acids Res 29:66–69.

52. Voorberg-van der Wel A, Zeeman AM, van Amsterdam SM, van den Berg A, Klooster EJ, Iwanaga S, Janse CJ, van Gemert GJ, Sauerwein R, Beenhakker N, Koopman G, Thomas AW, Kocken CHM. 2013. Transgenic Fluorescent Plasmodium cynomolgi Liver Stages

Enable Live Imaging and Purification of Malaria Hypnozoite-Forms. PLoS One 8:e54888.

53. Gural N, Mancio-Silva L, Miller AB, Galstian A, Butty VL, Levine SS, Patrapuvich R, Desai SP, Mikolajczak SA, Kappe SHI, Fleming HE, March S, Sattabongkot J, Bhatia SN. 2018. In Vitro Culture, Drug Sensitivity, and Transcriptome of Plasmodium Vivax Hypnozoites. Cell Host Microbe 23:395-406.e4.

54. Zanghì G, Vembar SS, Baumgarten S, Ding S, Guizetti J, Bryant JM, Mattei D, Jensen ATR, Rénia L, Goh YS, Sauerwein R, Hermsen CC, Franetich JF, Bordessoulles M, Silvie O, Soulard V, Scatton O, Chen P, Mecheri S, Mazier D, Scherf A. 2018. A Specific PfEMP1 Is Expressed in P. falciparum Sporozoites and Plays a Role in Hepatocyte Infection. Cell Rep 22:2951–2963.

55. Voorberg-van der Wel A, Roma G, Gupta DK, Schuierer S, Nigsch F, Carbone W, Zeeman AM, Lee BH, Hofman SO, Faber BW, Knehr J, Pasini E, Kinzel B, Bifani P, Bonamy GMC, Bouwmeester T, Kocken CHM, Diagana TT. 2017. A comparative transcriptomic analysis of replicating and dormant liver stages of the relapsing malaria parasite plasmodium cynomolgi. Elife 6:e29605.

643 **FIGURES AND LEGENDS**

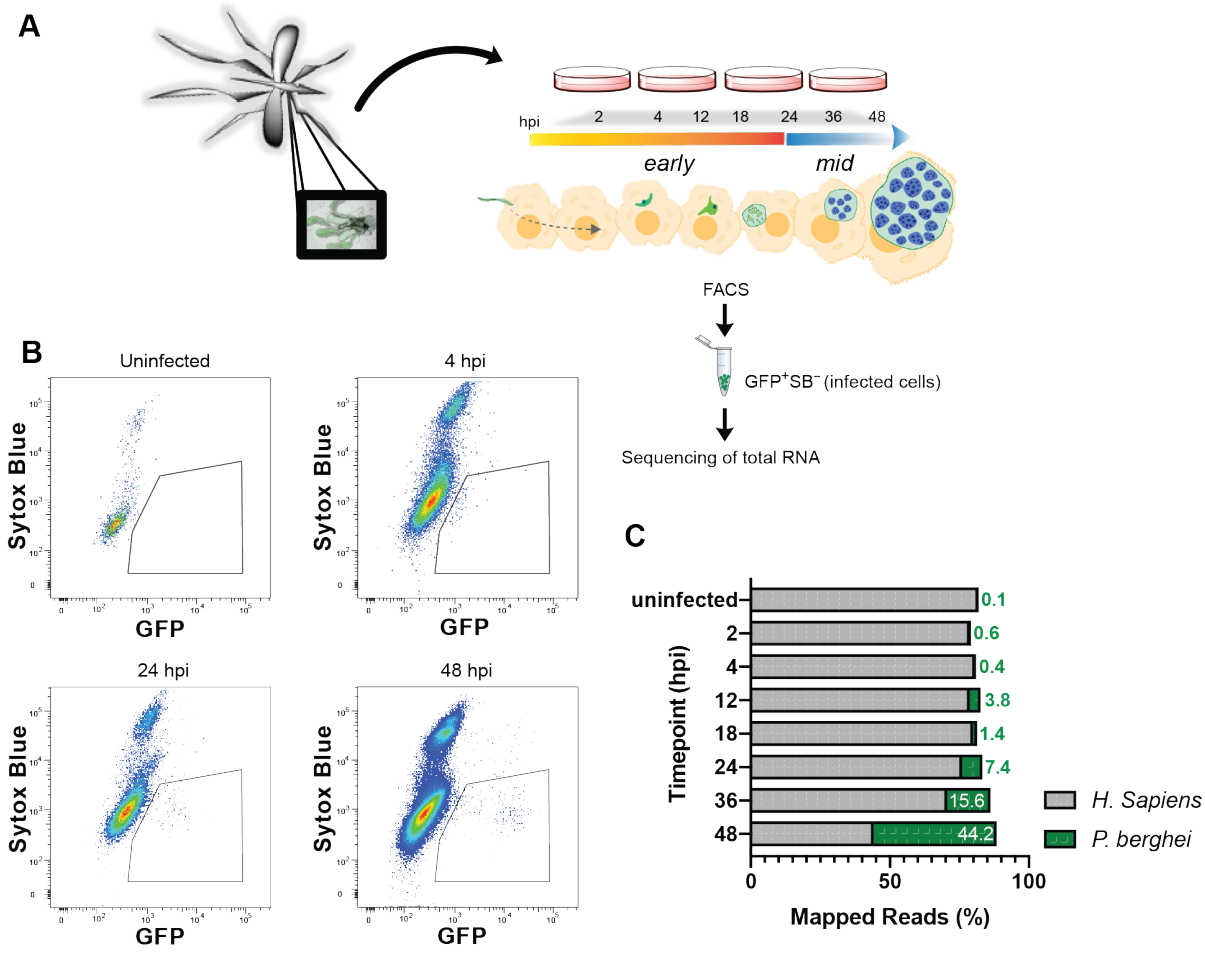

644

645 **Figure 1. Experimental design for RNA-seq of early and mid-stages of *P. berghei* liver**
646 **infection. (A)** Experimental design schematic. Female *Anopheles* mosquitoes were dissected and
647 GFP-expressing *P. berghei* sporozoites were harvested to infect HuH7 or HepG2 cells. Cells were
648 harvested 2, 4, 12, 18, 24, 36 or 48 hpi and FACS-sorted to enrich viable *P. berghei*-infected cells
649 for RNA collection. **(B)** Representative flow cytometry fluorescence dot plots indicating the
650 population of $GFP^{+}SytoxBlue^{-}$ cells that were collected at various time points. **(C)** Relative
651 percentage of transcripts mapping to *P. berghei* or *H. sapiens* at various times post infection.

652 Uninfected samples correspond to naïve uninfected cells treated with debris from dissected male

653 *Anopheles* mosquito salivary glands. Data are median of 2–5 biological replicates.

654

655

656

657

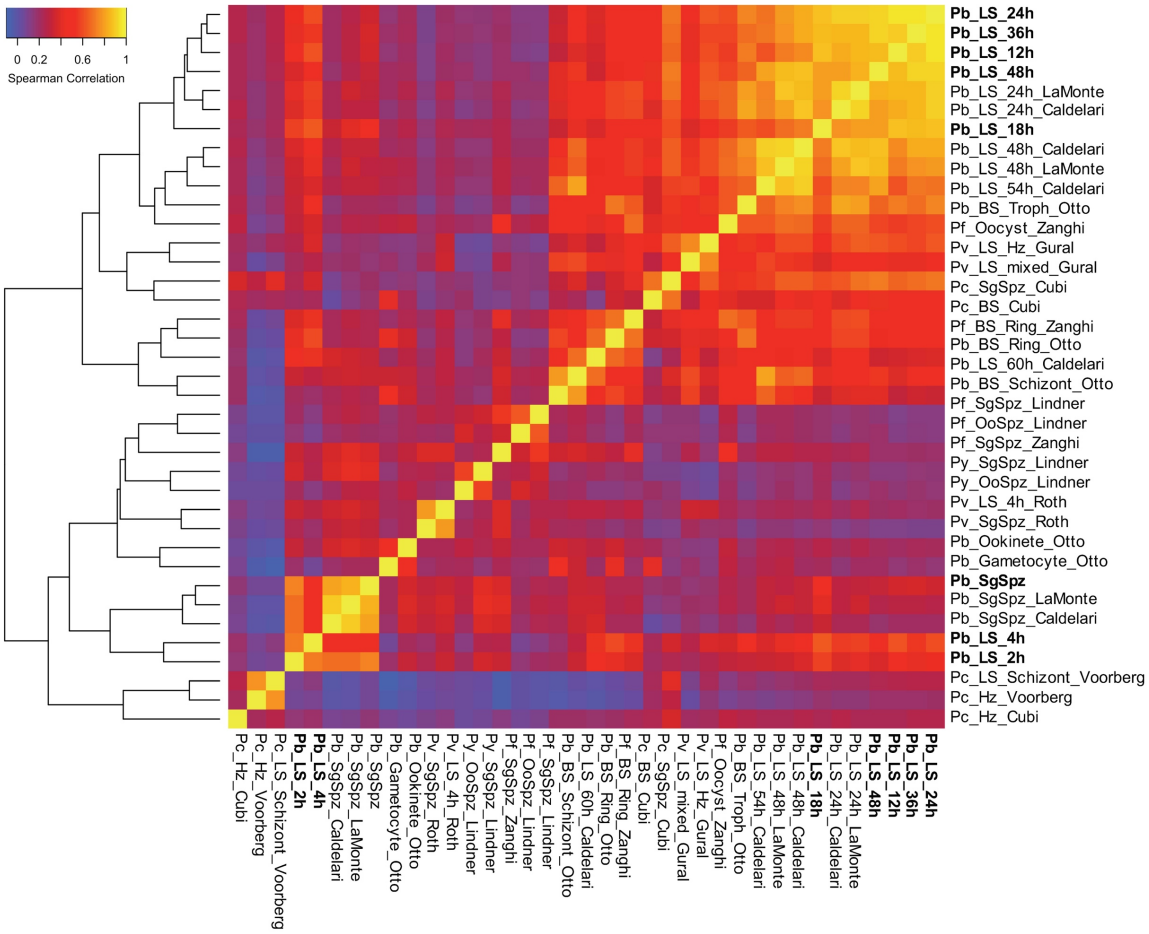

658

659 **Figure 2. Overview of *Plasmodium* transcriptome analyses.** Hierarchical clustering of gene
660 expression datasets from different stages of the *Plasmodium* life cycle (7, 8, 26, 32, 34, 52–54).
661 Datasets generated in this study are in bold. Clustering is based on Spearman correlation
662 coefficients calculated and plotted using R. Refer to Table S1 for information regarding the
663 datasets used to generate this figure.

664

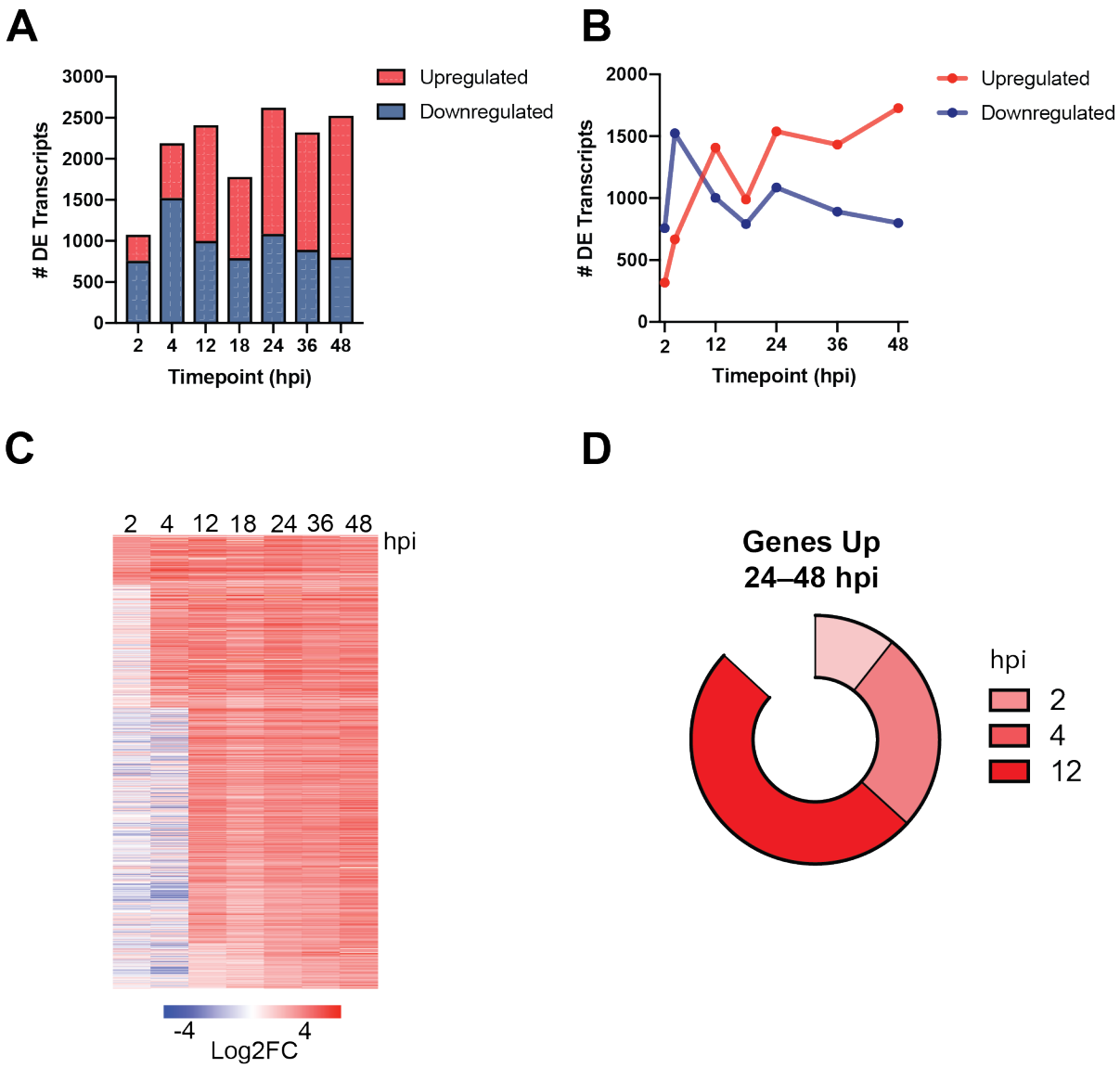

Figure 3. Dynamic gene regulation throughout liver-stage *P. berghei* development. Total **(A)** and upregulated (red)/ downregulated (blue) **(B)** differentially expressed (DE) transcripts ($q <$ 0.01) shown at each time point. **(C)** Expression profiles of 1,197 genes upregulated at 24, 36 and 48 hpi ordered based on the timepoint they were first observed to be upregulated. Expression is shown as the Log2 fold change vs sporozoite samples. **(D)** The proportion of genes that are upregulated throughout late stage development (24, 36 and 48 hpi) are divided by when they are first observed to be upregulated (2, 4 or 12 hpi).

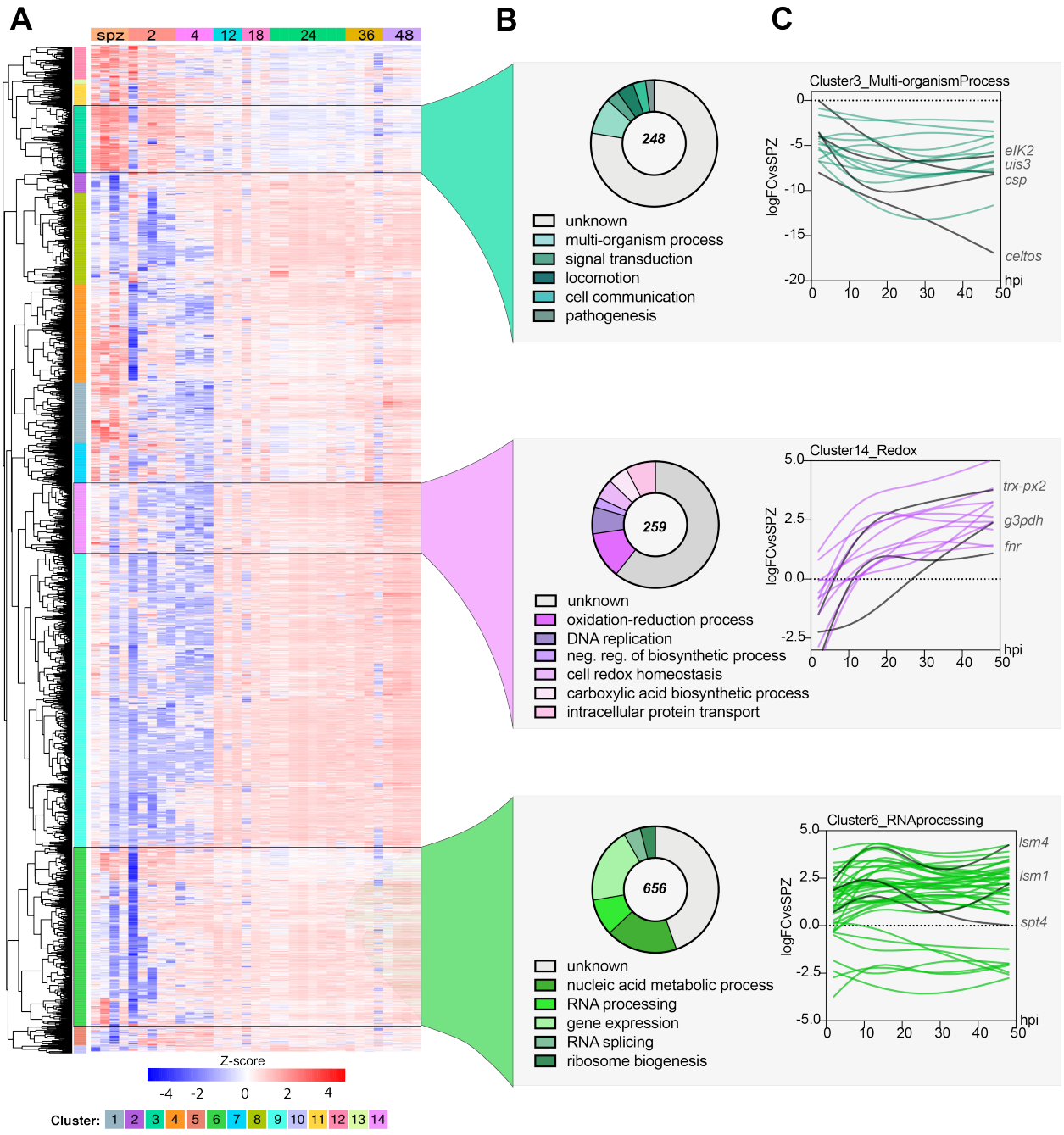

673

674 **Figure 4. Co-expression analysis identifies enriched processes during *P. berghei* development**

675 **in hepatocytes. (A)** Hierarchical clustering using a correlation distance with complete linkage of

676 all genes significant (FDR <= 5%) in at least one of the analyses. Gene expression is z-score

677 transformed. **(B)** GO Enrichment analysis (biological process) of enriched clusters 3, 14 and 6

678 shown. Representative GO terms ($p < 0.01$) and their respective number of genes (pie chart) are

679 shown. Total number of genes in each cluster is shown at the center of the pie chart. **(C)** Spline
680 models of gene expression data for all the genes in the top-scoring GO term in each cluster. Key
681 genes in each group and their expression patterns are highlighted in red. Refer to **Data S3** for
682 complete GO analysis of all clusters.

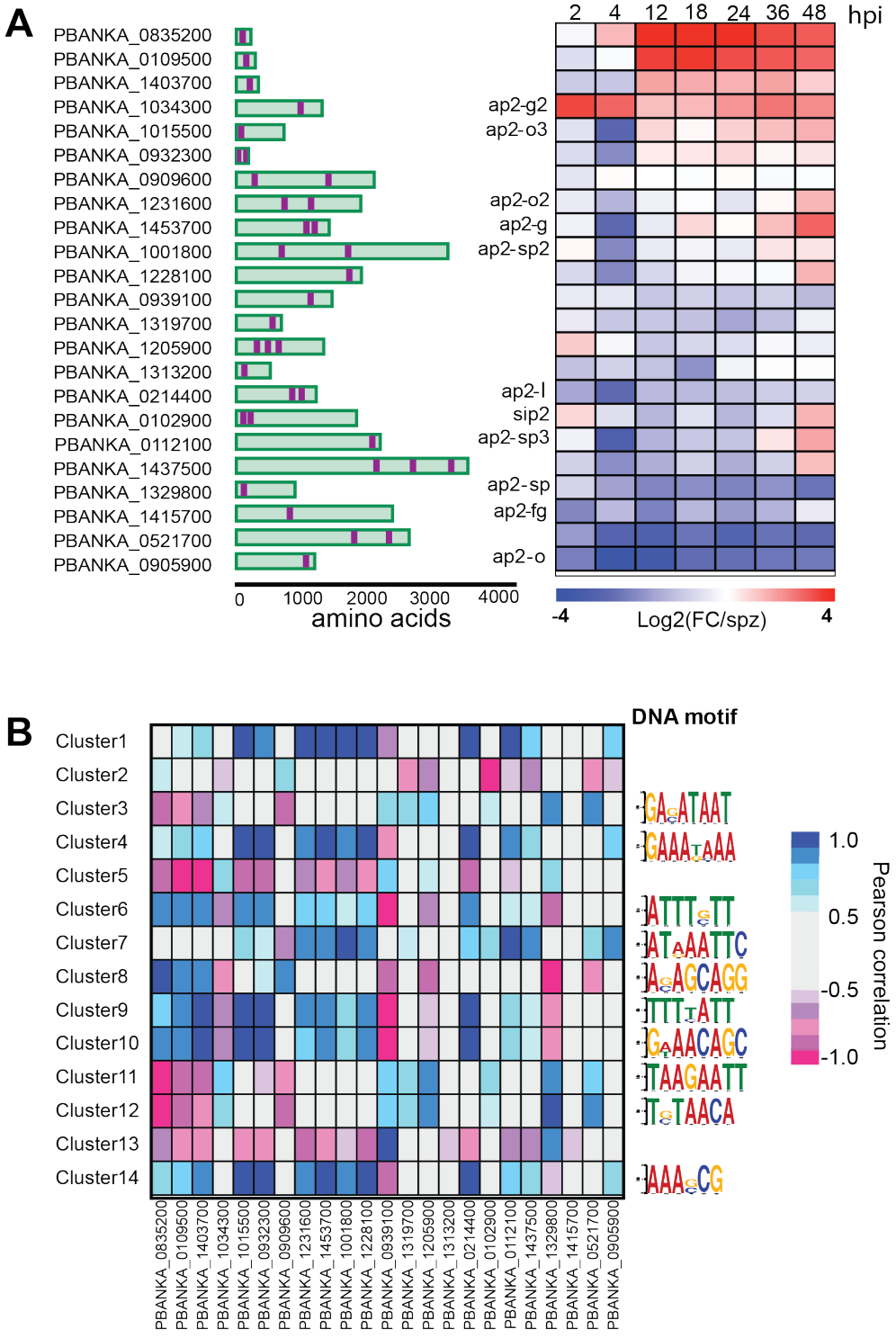

683

684 **Figure 5. Expression of *P. berghei* AP2 transcription factors in the liver stage. (A)** Gene IDs

685 of the 26 AP2 transcription factors in the *Pb* genome, their respective protein architecture

686 schematic (with AP2 displayed in purple) and their corresponding expression as the log2 fold

687 change vs spz at each time point in the LS. **(B)** Heatmap of Pearson correlations between AP2
688 transcription factors and the average expression of all genes in each cluster (left). The top most
689 enriched DNA motif for each cluster discovered through the DREME pipeline is shown (right).
690 Refer to **Data S3** for the complete set of motifs and their respective enrichment score.
691
692